E. G. Lean
M. L. Dakss
C. G. Powell

Efficiencies and Bandwidths of Intracavity Acousto-optic Devices

Abstract: Acousto-optic devices based on isotropic and anisotropic acoustic Bragg diffraction will be discussed in terms of their efficiency and bandwidth. The conflicting requirements on the width W of the acoustic column with regard to efficiency and bandwidth determine the basic limitations of the devices. A scheme using the acousto-optic devices within a flat-field conjugate (FFC) angularly degenerate laser cavity has been experimentally demonstrated. The bandwidth of the new scheme is limited by the field angle of the FFC cavity instead of by W^{-1}. The width W can be made as large as possible to increase the diffraction efficiency without decreasing the bandwidth. The new scheme provides means for high efficiency and large bandwidth in optical deflection and signal processing systems.

Introduction

Acousto-optic devices have become increasingly important for laser beam control in such applications as display, beam deflection and optical signal processing. For example, Korpel et al.[1] reported a television display scheme with a 200-spot-diameter resolution using Bragg diffraction of light from a steerable 30-MHz sound column in water. Lean et al.[2] demonstrated a scheme for continuously deflecting a laser beam through an angle of 4° by acoustic Bragg diffraction from a shear wave column in a birefringent crystal of sapphire. The scheme was capable of deflecting an optical beam through 1000 resolvable spots by tuning the shear wave column from 1.28 to 1.83 GHz. Optical pulse compression and signal processing techniques using Bragg diffraction of light from acoustic microwaves have also been reported by Collins et al.,[3] Schulz et al.[4] and Whitman et al.[5] The success of these acousto-optic devices is due to improvement in the fabrication techniques for broadband efficient microwave acoustic transducers[6] and also to the discovery of materials that have excellent acoustic and optical properties and that have large photoelastic constants.[7] Broadband, efficient ZnO thin film transducers,[8] which have 10-dB coupling loss over a 600-MHz bandwidth, provide a very large absolute bandwidth for acoustic devices. Materials with large photoelastic constants have improved efficiency.

The authors are located at the IBM Thomas J. Watson Research Center, Yorktown Heights, New York 10598.

The essential requirements of acousto-optic devices either for deflection or for signal processing applications are a large bandwidth, a high efficiency and a high speed. These properties are discussed in the next section. We point out that the bandwidth of an isotropic acoustic device acting on a collimated incident light beam is inversely proportional to the width W of the acoustic column while the diffraction efficiency is directly proportional to W. This gives conflicting requirements on W with regard to the bandwidth and to the efficiency. In addition, discussions of the efficiency and bandwidth of anisotropic acousto-optic devices are included and similar conflicting requirements are shown to exist.

The conflicting requirements with regard to W occur only for the case in which both the incident light beam and the acoustic beam are collimated. By using a series of acoustic transducers to steer the acoustic beam, it has been shown that the Bragg condition can be satisfied over a large bandwidth without decreasing the acoustic beam width.[2,5] Techniques for fabricating the transducer array, however, may limit a practical acoustic beam steering deflector to the lower end of the UHF region. In the third section of this paper a scheme using intracavity acousto-optic devices within an angularly degenerate laser cavity is described. This scheme provides another means for overcoming the conflict in the requirements on W and permits large efficiencies together with large bandwidths. The results of an experiment demonstrating these principles

and the advantages of using such acousto-optic devices for deflection and signal processing applications are discussed in the final section.

Properties of acousto-optic devices

In this section the efficiency and spot resolution potential of acousto-optic devices will be discussed. A collimated incident light beam and a collimated acoustic column will always be assumed.

• *Efficiency*

At microwave acoustic frequencies the interaction of light and acoustic waves can be described as acoustic Bragg diffraction.[9] Under the assumption that the intensity I_1 of the incident light is not decreased substantially in the process of diffraction, as is true in most existing devices, the diffraction efficiency $\mu = I_2/I_1$, where I_2 is the intensity of the first-order diffracted light, can be shown[10] to be given by

$$\mu = \beta P_{ac} W/H, \tag{1}$$

where P_{ac} is the acoustic power, W is the width of the acoutic beam, H is the height of the acoustic beam and

$$\beta = (\pi^2 n^6 p^2)/(2\lambda_0^2 \rho v^3) \tag{2}$$

is a constant of the acoustic medium. In the expression for β, n is the index of refraction, λ_0 is the wavelength of the incident beam in vacuum, ρ is the density of the medium, v is the acoustic wave velocity, and p is the photoelastic constant. The proportionality of the diffraction efficiency to the column width W, referred to above, is seen from Eq. (1). This expression holds for both isotropic and anisotropic diffraction (see the next section).

Materials with a large value of β such as lithium niobate ($LiNbO_3$) and lithium tantalate ($LiTaO_3$) have been studied extensively.[11] $LiNbO_3$ has been found to have a value of β of the order of 10^{-2} at optical frequencies; in this crystal, for an acoustic beam in which $W = H$, one watt of acoustic power is required for a diffraction efficiency of one percent. The available acoustic power is limited by the electrical breakdown threshold of the transducer. CdS wide-band thin film transducers having a 16-dB electrical-to-acoustic power conversion efficiency over a 1400-MHz bandwidth and capable of handling a 46-W peak acoustic power have been reported.[12] Techniques for fabricating efficient wide-band transducers have improved rapidly so that suitably high cw acoustic power should become possible.

• *Bandwidth*

Bragg diffraction of light by acoustic microwaves is a parametric interaction process in which "phase matching" (momentum conservation) is a basic requirement.[10] Phase matching requires that the vector sum of the three wave vectors be zero, i.e., $\mathbf{k}_2 = \mathbf{k}_1 \pm \mathbf{K}$, where $\mathbf{K}$ is the wave vector for the acoustic wave and $\mathbf{k}_1$ and $\mathbf{k}_2$ are the wave vectors for the incident and diffracted light waves, respectively. There are two types of acoustic Bragg diffraction of light, isotropic[9] and anisotropic.[13] For isotropic diffraction both the incident light and diffracted light encounter the same index of refraction in the medium and there is no polarization change between the incident and diffracted light; in this process $|\mathbf{k}_1| = |\mathbf{k}_2|$. For anisotropic diffraction the indices of refraction are different for the incident and diffracted light (different polarization) and $|\mathbf{k}_1| \neq |\mathbf{k}_2|$. We shall briefly discuss bandwidths and the number of resolvable spots expected for the two types of diffraction.

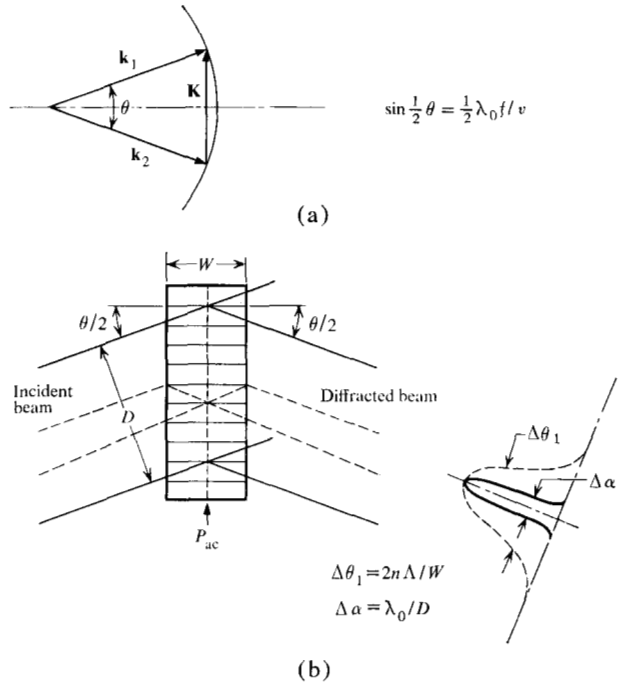

Figure 1 Isotropic acoustic Bragg diffraction: (a) **k**-vector relationship for phase matching in isotropic crystals and (b) schematic diagram showing isotropic diffraction of light by an acoustic column; $\Delta\theta_1$ is the angular bandwith and $\Delta\alpha$ is the spot size of the diffracted light.

Isotropic diffraction

To treat the case of isotropic diffraction we first assume that an incident light beam of intensity I_1 is deflected by an isotropic Bragg cell with an acoustic column of width W and wavelength Λ (see Fig. 1). The diffracted intensity I_2 will be maximum when the phase matching condition holds and when the angle $\theta/2$ that the incident beam makes with the acoustic wave front is the same as the angle the diffracted beam makes with the wave front.

This (Bragg) condition is given by

$$\sin \tfrac{1}{2}\theta = \tfrac{1}{2}\lambda f/v, \tag{3}$$

where the angle $\frac{1}{2}\theta$ is measured in the Bragg cell and where f is the frequency of the acoustic wave; $\lambda = \lambda_0/n$ is the wavelength of the incident light in the medium with an index of refraction n. The angular bandwidth for an isotropic Bragg cell has been derived from the momentum conservation requirement.[10] The result is that it is possible to deflect a collimated laser beam entering a Bragg cell at the Bragg angle given by Eq. (3) over an angular bandwidth (measured outside the Bragg cell)

$$\Delta\theta_1 = 2n\Lambda/W \tag{4}$$

by correspondingly adjusting the acoustic frequency over a bandwidth

$$\Delta f_1 = 2n(v/\lambda_0)\Lambda/W. \tag{5}$$

For both Eqs. (4) and (5) bandwidth is defined between the −4-dB points of the intensity distribution. The finite angular and frequency bandwidths occur as a result of the finite width of the acoustic column.

The bandwidth for isotropic diffraction can be understood easily using simple diffraction theory (see Fig. 1). Each spatial period of the acoustic wave diffracts part of the incident light. An acoustic wavefront can be thought of as a "reflector" with an effective aperture

$$d = W \sin \tfrac{1}{2}\theta \tag{6}$$

equal to the width of the incident light beam section (e.g., that between the dotted lines in Fig. 1) intercepted by one such wavefront. Reflection from a single wavefront would produce a far-field diffraction pattern containing a central maximum of angular bandwidth

$$\Delta\theta_1 = n\lambda/d = 2n\Lambda/W. \tag{7}$$

The incident light beam (of diameter D) covers many acoustic wave periods and the light waves diffracted from different periods interfere with each other.

This interference leads to a series of diffraction maxima of width

$$\Delta\alpha = \lambda_0/D \tag{8}$$

separated by the angle λ_0/Λ. From Eq. (7) this interference spacing is much larger than $\Delta\theta_1$ so that only one diffracted spot lies within the central peak of the diffraction envelope for a single acoustic wavefront. At the acoustic frequency for which the Bragg condition holds, the deflected beam is centered in this peak and has maximum intensity. As the frequency is varied the peak is scanned within the envelope. The number N of resolvable spots, a primary property of acousto-optic devices used in deflection applications, is given by the ratio of the envelope width $\Delta\theta_1$ to the spot width $\Delta\alpha$ or, using Eqs. (7) and (8),

$$N = 2n(D/\lambda_0)\lambda/W. \tag{9}$$

By using Eq. (5), Eq. (9) can be reduced to the well-known form

$$N = \tau\,\Delta f, \tag{10}$$

where

$$\tau \equiv D/v \tag{11}$$

is the transit time of the acoustic wave across the laser beam of diameter D. We note that τ is the minimum switching time for random access deflection. The time-bandwidth product N as given by Eq. (10) is also the compression-ratio criterion for optical pulse compression techniques.[3]

It can be seen from Eq. (9) that the number of resolvable spots for an isotropic deflector is inversely proportional to the width of the acoustic column and we noted earlier that the diffraction efficiency was directly proportional to this width. Thus there are conflicting requirements on W with regard to the important properties of number of resolvable spots and efficiency of an isotropic acousto-optic deflector.

Anisotropic diffraction

For the case of anisotropic Bragg diffraction the incident and diffracted light beams see different refractive indices. It can be shown that by properly adjusting the acoustic wave vector $\mathbf{K}$ in an optically uniaxial crystal it is possible to diffract a light beam that is incident on the Bragg cell at an angle θ and is traversing the cell with extraordinary polarization into a beam with ordinary polarization that is propagating along a direction parallel to the acoustic wave fronts. Figure 2 shows a typical configuration for such anisotropic diffraction. The Bragg condition for this anisotropic diffraction is different from that of the isotropic case and is given by [14]

$$\sin\theta = \lambda f_0/v, \tag{12}$$

where θ is the angle between the incident and diffracted beams in the crystal and

$$f_0 = v/\Lambda_0 = \sqrt{2nB}\,(v/\lambda_0) \tag{13}$$

is the central acoustic frequency; at this frequency, which is determined by the optical wavelength λ_0 and by properties of the acoustic medium including its birefringence B (we assume a uniaxial medium), the diffracted light is traveling in a direction parallel to the acoustic wave front.

The angular bandwidth and the number of resolvable spots of the anisotropic deflector can be calculated easily. As the acoustic frequency is changed from f_0 to $f_0 + \Delta f$, the diffracted light has to leave the acoustic column at an angle θ_2 (not zero) with respect to the acoustic wave fronts to satisfy the phase-matching con-

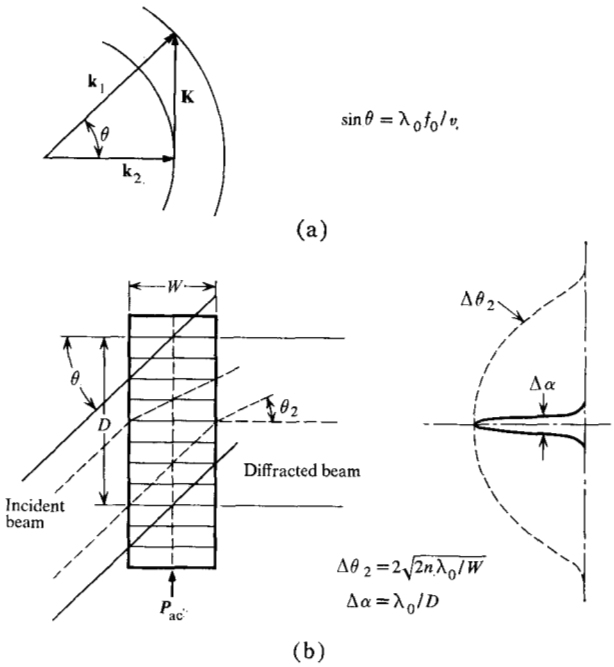

Figure 2 Anisotropic acoustic Bragg diffraction of an obliquely incident light beam: (a) **k**-vector relationship for phase matching in an optically uniaxial crystal and (b) schematic diagram showing anisotropic diffraction of an obliquely incident light beam by an acoustic column; $\Delta\theta_2$ is the angular bandwidth and $\Delta\alpha$ is the spot size of the diffracted light.

dition. From Fig. 2 the condition for the maximum value of θ_2 before destructive interference from the acoustic grating reduces the diffracted light to an intensity 4 dB below the intensity at $\theta_2 = 0$ is given by

$$k_1 W \cos\theta - k_2 W \cos\theta_2 = 2\pi, \tag{14}$$

where $k \equiv |\mathbf{k}|$.

Expanding $\cos\theta_2$ for small θ_2 and using the phase-matching condition for anisotropic Bragg diffraction, i.e.,

$$k_1 \cos\theta - k_2 = 0, \tag{15}$$

which can be shown using Fig. 2a to be equivalent to Eq. (12), we obtain the following relation for θ_2 at the −4-dB point:

$$\theta_2 = \sqrt{2\lambda/W}. \tag{16}$$

Because the variation in intensity with θ_2 is approximately symmetric about the value $\theta_2 = 0$, the total angular bandwidth (measured outside the crystal) for the anisotropic deflector is

$$\Delta\theta_2 = 2n\theta_2 = 2\sqrt{2n\lambda_0/W}. \tag{17}$$

The spot size $\Delta\alpha$ of the diffracted light for an incident beam having a diameter D that covers a large number of acoustic wavelengths is given by Eq. (8). The number of resolvable spots N, which is given by the ratio of $\Delta\theta_2$ to $\Delta\alpha$, can be written as

$$N = 2D\sqrt{\frac{2n}{\lambda_0 W}} \tag{18}$$

and can again be reduced to $N = \tau\Delta f$ if

$$\Delta f_2 = 2v\sqrt{\frac{2n}{\lambda_0 W}} \tag{19}$$

is the corresponding frequency bandwidth for the anisotropic deflector. We recall from the beginning of this section that the efficiency for anisotropic diffraction is linearly proportional to the width of the acoustic column for constant acoustic power input. The number of resolvable spots [Eq. (18)] is inversely proportional to $\sqrt{W}$. The conflicting requirements on W therefore hold true for this anisotropic case.

There is a second type of anisotropic Bragg diffraction in which the incident light beam is parallel to the acoustic wave front and the diffracted light exits at an angle θ given by the Bragg condition

$$\tan\theta = \lambda/\Lambda_0 = \lambda f_0/v, \tag{20}$$

where f_0 is the central acoustic frequency as given in Eq. (13). The typical configuration for such anisotropic diffraction with a normally incident light beam is shown in Fig. 3. The effective aperture d for the single wave front having width W is

$$d = W\sin\theta. \tag{21}$$

For small θ the angular bandwidth of the device is given by

$$\Delta\theta_3 = n\lambda/d = n\Lambda_0/W \tag{22}$$

and the frequency bandwidth is given by

$$\Delta f_3 = n(v/\lambda_0)\Lambda_0/W. \tag{23}$$

Notice that there is a difference of a factor of two between Eqs. (4) and (22) and between Eqs. (5) and (23).

The number of resolvable spots can be shown from Eqs. (8) and (22) to be inversely proportional to W, while the diffraction efficiency is directly proportional to W. Thus we see that the conflicting requirements on W hold for anisotropic diffraction as well as for isotropic diffraction.

Acousto-optic diffraction within angularly degenerate laser cavities

In this section we describe a scheme for acousto-optic signal processing that is potentially highly efficient and has large bandwidth. The scheme involves placing an acoustic Bragg cell in an angularly degenerate laser cavity. We use an isotropic cell and a flat-field conjugate (FFC) laser cavity[15] in this description since these were used to

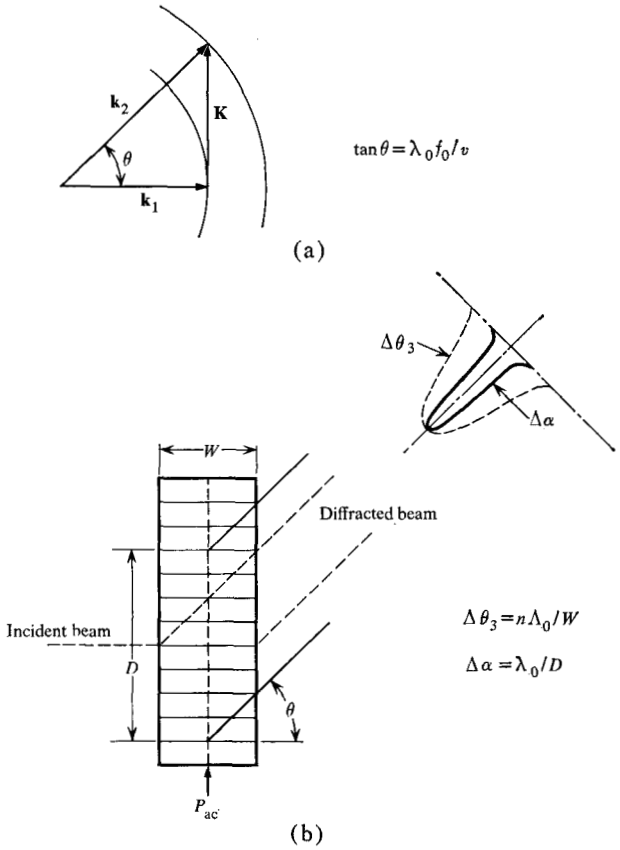

Figure 3 Anisotropic acoustic Bragg diffraction with a normally incident light beam: (a) **k**-vector relationship for phase matching in an optically uniaxial crystal and (b) schematic diagram showing anisotropic diffraction of a normally incident light beam by an acoustic column; $\Delta\theta_3$ is the angular bandwidth and $\Delta\alpha$ is the spot size of the diffracted light.

demonstrate the principles involved. The FFC cavity (Fig. 4) consists of two lenses separated by the sum of their focal distances, an active laser medium, an acoustic Bragg cell at the common focal plane of the lenses and two flat end-mirrors located in the noncommon focal planes of the lenses. Such a cavity can support a degenerate set of transverse modes; each mode of this set is focused on a different spot on one end mirror and on the corresponding conjugate spot on the other end mirror. At the acoustic cell each of the transverse modes is collimated, but is incident at a different angle $\alpha - \frac{1}{2}\phi$ with respect to the acoustic wave front. Here α is the angle between the acoustic wave front and the axis of the FFC cavity and $\frac{1}{2}\phi$ is the angle between the chief ray of the mode and this axis. The maximum value ϕ_{max} of ϕ can be determined by the dimensions of the active medium if the lenses are assumed to be perfect.

We first consider the use of such a scheme for deflection applications. A small number of transverse modes in the FFC cavity that satisfy (or nearly satisfy) the Bragg condition will be selectively diffracted upon creating acoustic waves with the proper frequency in the Bragg cell. The diffracted beam can be coupled out to form the laser output beam without passing through the end mirrors, which can be of ultra-high reflectivity. Then, as the acoustic frequency is varied, different transverse modes will be selected and the laser output will, in effect, be scanned. The angular bandwidth of the output is now approximately equal to the maximum field angle ϕ_{max} of the FFC cavity and is no longer limited by W. However, W now determines the selectivity $\Delta\theta = n\Lambda/W$ of the Bragg cell since $\Delta\theta$ is the angular spread over which

Figure 4 Acousto-optic cell within a flat-field conjugate laser cavity (schematic diagram).

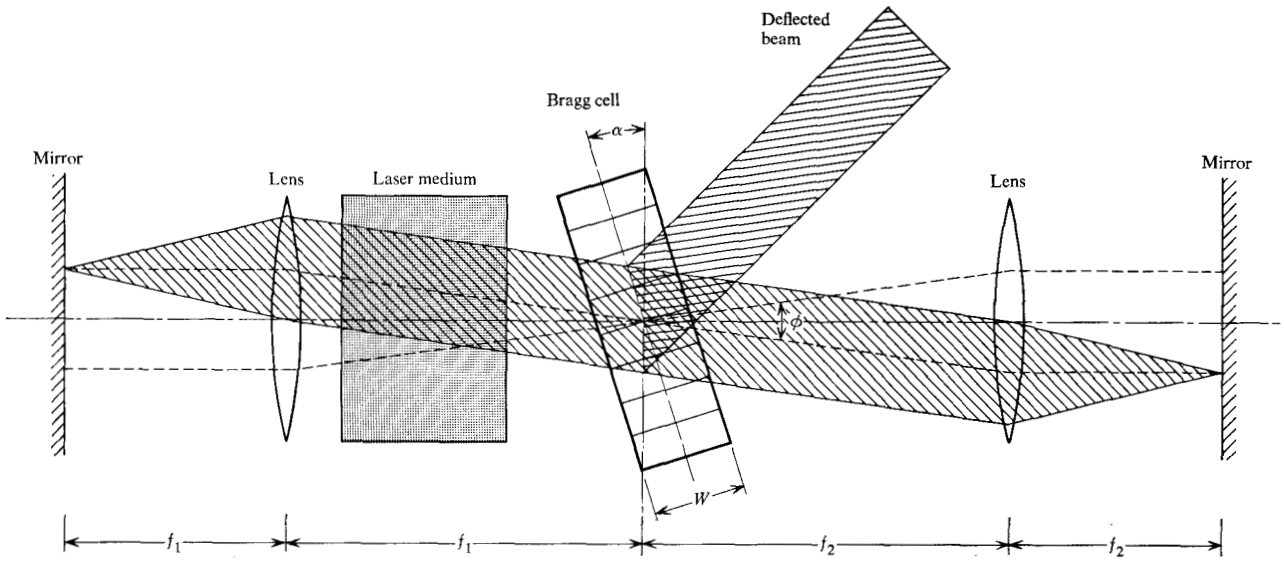

transverse modes will be diffracted. The number of resolvable spots in the present deflection scheme is given by $N = \phi_{max}/\Delta\theta$ or by

$$N = (\phi_{max}/n)(W/\Lambda). \quad (24)$$

Thus W has to be increased to increase the number of resolvable spots and improve the selectivity. At the same time the efficiency of Bragg diffraction will increase and the required acoustic driving power consequently will decrease. There are no conflicting requirements in this case.

If the system is used for optical pulse compression,[3] all of the transverse modes inside the laser cavity contribute to the diffracted signal. In this case the increase in frequency bandwidth Δf due to the FFC cavity configuration helps in obtaining a shorter compressed pulse (the pulse width is $\Delta t = 1/\Delta f$) and consequently a better resolution. At the same time a large W can be used to enhance the diffraction efficiency and reduce the required acoustic driving power.

It should be noted that in the case of deflection the diffracted output of the laser decreases as N increases if each of the transverse modes is stimulated to emit independently. However, the output could be increased if there were coupling of power from the high-Q recirculating modes into the output modes to produce, for example, so-called "super mode" operation.[16]

Experimental results and implications

The first experiment demonstrated the angular and frequency bandwidths of isotropic and anisotropic acoustic Bragg cells operated with a collimated incident light beam. For the anisotropic cell, measurements were made only for the case in which the incident beam was parallel to the acoustic wavefront. The second experiment demonstrated the increase in bandwidth of an isotropic Bragg cell operated within a FFC cavity and the optimum coupling condition for the Bragg cell within a FFC Cavity.

• *Measurement of angular and frequency bandwidths*

In the measurement of the bandwidths of an isotropic Bragg cell and of an anisotropic Bragg cell having the incident beam normal to the cell we used a $LiTaO_3$ crystal[17] operating in the shear wave mode S_4; in this mode, the acoustic wave propagates along the y axis of the crystal with the particle motion parallel to the z axis. $LiTaO_3$ is a positive uniaxial crystal having non-zero photoelastic constants p_{24} and p_{44}. We could conveniently use the same acoustic mode S_4 for both isotropic and anisotropic diffraction. For isotropic diffraction the photoelastic constant p_{24} is involved, while for anisotropic diffraction the constant p_{44} is involved.[14]

The bandwidths of the Bragg cell were determined by measuring the intensity and propagation direction of the diffracted beam as a function of the acoustic frequency

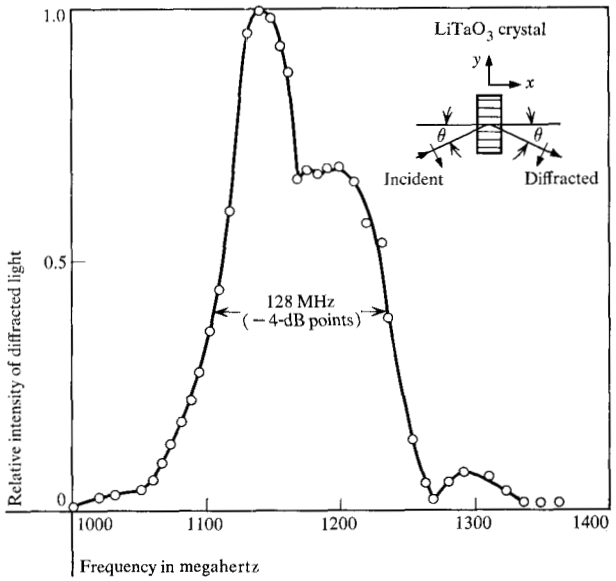

Figure 5 Plot of the measured relative intensity of the diffracted light beam vs. acoustic frequency in a $LiTaO_3$ Bragg cell for isotropic diffraction.

with the collimated incident beam fixed in direction with respect to the Bragg cell. A He-Ne gas laser emitting at 6328 Å was used as a source. The acoustic mode S_4, for which the acoustic velocity $v = 5.53 \times 10^5$ cm/sec, had a width of 0.15 cm. Figure 5 shows the relative diffracted intensities plotted vs. the acoustic frequency for the isotropic diffraction case; the frequency for maximum diffracted intensity was 1.15 GHz in this case, in agreement with the value calculated from Eq. (3) for the 7.8° angle of incidence used. The measured bandwidth was 128 MHz while the value calculated from Eq. (5) is 123 MHz. Figure 6 shows a plot of the measured relative diffracted intensity vs. the acoustic frequency for the anisotropic diffraction case; again the acoustic frequency for maximum diffracted wave intensity was 1.15 GHz. This is in agreement with the value of 1.15 GHz calculated from Eq. (13) with the values $n_0 = 2.176$, $B = 0.0042$, and $\lambda_0 = 6328$ Å. The measured bandwidth in this case was 64 MHz while the value calculated from Eq. (23) is 62 MHz. It should be noted that the factor of two predicted by Eqs. (5) and (23) for isotropic diffraction and anisotropic diffraction with normally incident beam is verified experimentally.

The bandwidth of the anisotropic diffraction with the incident beam oblique with respect to the acoustic wave front has also been verified experimentally. Using a slow shear wave column of 0.175-cm width in an anisotropic sapphire Bragg cell, Lean et al.[2] measured a bandwidth of 550 MHz, which agrees with the value calculated from Eq. (19).

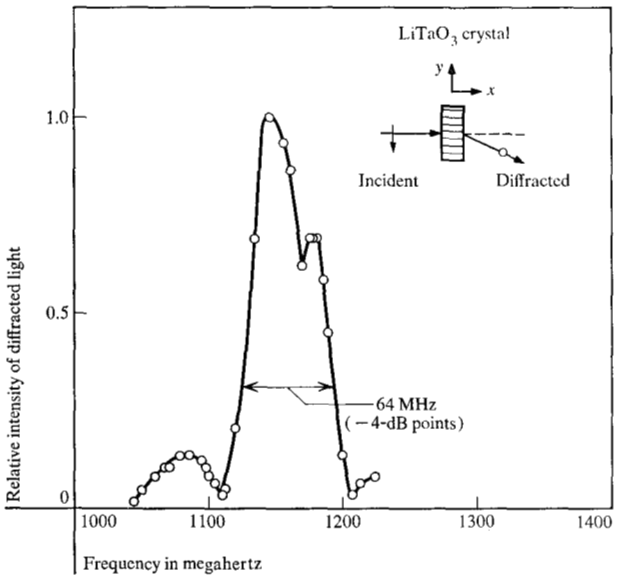

Figure 6 Plot of the measured relative intensity of the diffracted light beam vs. acoustic frequency in a $LiTaO_3$ Bragg cell for anisotropic diffraction at normal incidence.

• *Bandwidth enhancement for isotropic diffraction in an angularly degenerate laser cavity*

In the second experiment a $LiNbO_3$ Bragg cell was used within a Nd:YAG laser cavity. The cell was operated in the shear wave isotropic diffraction mode and utilized the photoelastic constant p_{66} at an acoustic frequency of approximately 1.1 GHz. The acoustic column width W was 0.45 cm. The bandwidth of this isotropic $LiNbO_3$ Bragg cell was first measured within a Nd:YAG laser cavity having one or few transverse modes; this was a flat-field cavity stabilized by the thermally induced lens in a 3-in. long by $\frac{1}{4}$-in. diameter YAG active medium (see the upper left sketch in Fig. 7). The experimental results are shown by the solid curve (a) in Fig. 7. The measured frequency bandwidth for the diffraction (between −4-dB points) was 20 MHz, while the value calculated from Eq. (5) is 16 MHz. The measured angular bandwidth was 16 min, while that calculated from Eq. (7) is 13 min. The discrepancy is probably due to the oscillation of more than one transverse mode in the cavity. For the experimental laser beam diameter (0.26 cm) the number N of resolvable spots calculated from the measured bandwidth and spot size is 8, while Eq. (24) indicates 10. The same $LiNbO_3$ Bragg cell was also used within the Nd : YAG laser in the FFC cavity configuration[18] as shown in Figs. 4 and 7b. The maximum field angle ϕ_{max} of the FFC cavity was measured as 1.5°. The angle α of Fig. 4 is 9.0° and the central acoustic frequency is 1.15 GHz. Figure 7 shows the measured dependence of relative diffracted intensities on the acoustic frequency of the $LiNbO_3$ Bragg cell within this FFC cavity (the dashed curve). The measured bandwidth was 2.1×10^2 MHz, which is equal to the value calculated from Eqs. (3) and (5) for a field angle of 1.5°. This represents an enhancement of bandwidth of more than a factor of 10. For deflection applications the number of resolvable spots N of the system is 11. With a proper active laser medium and with proper lenses it is possible to increase ϕ_{max} in the FFC cavity to 10°, causing the bandwidth of the system to be 1400 MHz. Together with the increase of W to 2.5 cm, the N of the system can exceed 500 when the operating acoustic frequency range is approximately 0.5 to 2 GHz. Anisotropic Bragg cells are expected to yield similar increases in efficiency and bandwidth when used within a FFC cavity. Since the Bragg cell provides the output coupling of the laser, the transverse mode that most nearly satisfies the Bragg condition will have the largest "loss" among all the transverse modes within the laser cavity. As the coupling is increased by increasing either the acoustic power or the column width, this "matched" mode will reach an optimal state; thereafter the output of the laser decreases with a further increase of the coupling. For other less well-matched modes, however, the energy coupled out will continue to increase. Thus the resolution of the system used in a deflection application will decrease when the output coupling exceeds the optimal value. To determine the optimum coupling condition, the $LiNbO_3$ Bragg cell was put within a FFC cavity having 2% excess gain. A few transverse modes were diffracted by the acoustic column of width 0.45 cm. By scanning

Figure 7 Plot of the measured relative intensity of the diffracted light beam vs. acoustic frequency for the case of an isotropic acousto-optic deflector in (a) a non-degenerate laser cavity and (b) a flat-field conjugate laser cavity. The inserts schematically indicate the experimental arrangements.

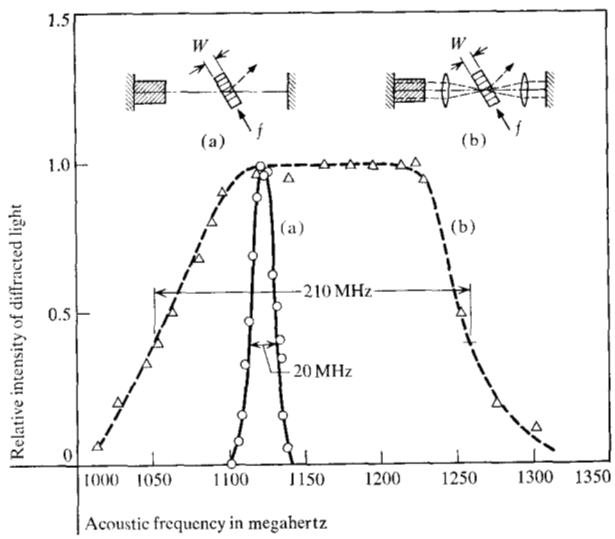

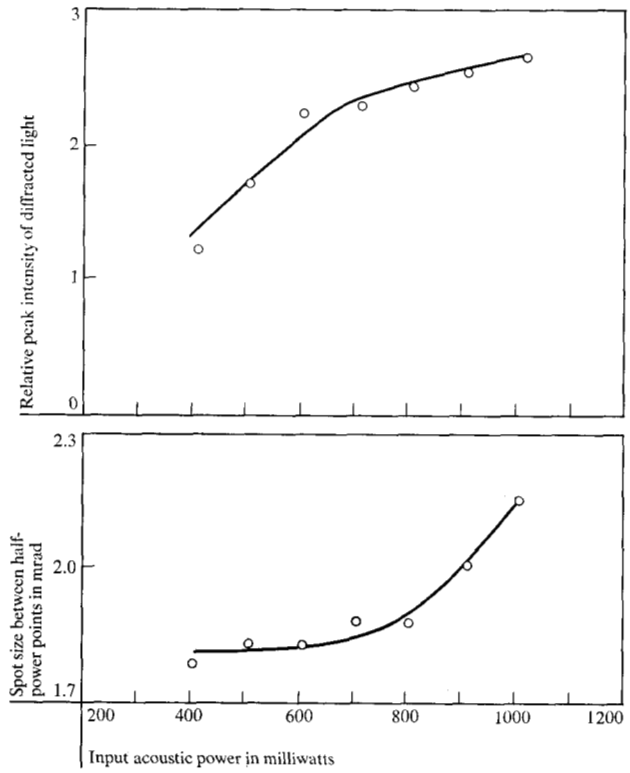

Figure 8 Intensity and spot size of the diffracted light beam output of an acousto-optic deflector in a flat-field conjugate laser cavity as a function of acoustic power input.

across the deflected beam with a photomultiplier apertured with a pinhole, we measured the spatial distribution of intensity in the deflected spot as a function of the coupling efficiency of the Bragg cell. Figure 8 shows the relative peak intensity and the spot size (between half-power points) as functions of input acoustic power or, equivalently, as functions of output coupling. Saturation effects are clearly seen. The optimal output coupling of the Bragg cell for this particular FFC cavity is 1.4% and the corresponding input acoustic power is 600 mW. The output power at optimum coupling can be increased by decreasing non-useful laser losses. The required acoustic power input can be decreased by using a wider acoustic column. For example, only 100 mW of acoustic power are required to diffract 1% of the laser intensity within the cavity if the acoustic width W is increased to 2.0 cm. The 100 mW of acoustic power required over the bandwidth of 210 MHz can be obtained easily using presently available thin film transducers driven by a transistorized rf power source.

Summary

We have demonstrated a scheme for acousto-optic diffraction within an angularly degenerate cavity that yields increases in both the absolute bandwidth and the efficiency over those in techniques involving diffraction of collimated laser beams. The large absolute bandwidth and high efficiency of devices using this scheme provide excellent potential for these devices in optical deflection and signal processing applications.

Acknowledgments

The authors thank R. V. Pole for his contributions in initiating the acousto-optic experiment with the FFC cavity, R. A. Myers for his helpful discussions and suggestions,[6] and H. J. Shaw of Stanford University for permission to use unpublished data on the $LiTaO_3$ crystal.

References

1. A. Korpel, R. Adler, P. Desmares and W. Watson, *Proc. IEEE* **54,** 1429 (1966).
2. E. G. H. Lean, C. F. Quate and H. J. Shaw, *Appl. Phys. Letters* **10,** 48 (1967).
3. J. H. Collins, E. G. H. Lean and H. J. Shaw, *Appl. Phys. Letters* **11,** 240 (1967).
4. M. B. Schulz, M. G. Holland and L. Davis, Jr., *Appl. Phys. Letters* **11,** 237 (1967).
5. R. Whitman, A. Korpel and S. Lotsoff, *Proceedings of the Symposium on Modern Optics,* J. Fox, Ed., Polytechnic Institute of Brooklyn, distributed by Interscience Publishers, New York, p. 243 (1967).
6. R. M. Malbon, D. J. Walsh and D. K. Winslow, *Appl. Phys. Letters* **10,** 9 (1967).
7. E. G. Spencer, P. V. Lenzo and K. Nassau, *Appl. Phys. Letters* **7,** 67 (1965).
8. R. M. Malbon, private communication.
9. C. F. Quate, C. D. W. Wilkinson and D. K. Winslow, *Proc. IEEE* **53,** 1604 (1965).
10. E. I. Gordon, *Proc. IEEE* **54,** 1391 (1966).
11. R. W. Dixon and M. G. Cohen, *Appl. Phys. Letters* **8,** 205 (1966).
12. W. A. Crofut, *Proc. IEEE,* **55,** 715 (1967).
13. R. W. Dixon, *IEEE J. Quant. Elec.* **QE-3,** 85 (1967).
14. E. G. H. Lean, *Microwave Laboratory Report 1543,* Stanford University (1967).
15. R. V. Pole, *J. Opt. Soc. Am.* **55,** 254 (1965).
16. S. E. Harris, *Proc. IEEE* **54,** 1401 (1966); a spatial version of super-mode operation was suggested by I. C. Chang and E. G. Lean (unpublished).
17. The bandwidth measurements on the $LiTaO_3$ crystal were made by E. G. Lean during 1967 in the Hansen Laboratory at Stanford University under the supervision of H. J. Shaw.
18. M. L. Dakss and C. G. Powell, *IEEE J. Quant. Elec.* **QE-4,** 130 (1968).

Received July 29, 1968